10th World Congress on Structural and Multidisciplinary Optimization
May 19 - 24, 2013, Orlando, Florida, USA

Convergence Improvement of Reliability-Based MultiobjectiveOptimization Using Hybrid MOPSO

Shoichiro KAWAJI[1] **and Nozomu Kogiso**[2]

[1,2] Department of Aerospace Engineering, Osaka Prefecture University, Sakai, Japan
10_kawaji_shoichiro@aero.osakafu-u.ac.jp, kogiso@aero.osakafu-u.ac.jp

1. Abstract
This study proposes the improvement method of computational efficiency for the hybrid-type multiobjective particle swarm optimization method (MOPSO) that the authors developed for the reliability-based multiobjective optimization (RBMO). The hybrid MOPSO integrates the constraint satisfaction technique using gradient information of constraints with a concept of the single-loop-single-vector method (SLSV). The constraint satisfaction technique consists of two functions: moving the design candidate with constraint violation to the feasible region based on the sensitivity of the violated constraints and to the feasible boundary using bi-section method. Some design candidates, however, take much computation with zigzag iterations until the candidate moves to feasible region. This study proposes the improvement method by eliminating the zigzag iterations based on an idea from the modified SLSV method or the conjugate mean value method proposed for resolving the convergence problem for the reliability-based optimization. The efficiency of the proposed method is demonstrated through several design problems by investigating the convergence and diversity of finding Pareto optimal solutions.
2. Keywords: Reliability-based multiobjective optimization, Hybrid multiobjective PSO, Single loop reliability-based optimization, Sensitivity analysis

3. Introduction
Multiobjective optimization method is widely applied to variety fields of engineering design problems. Especially, the evolutionary optimization algorithms are widely conducted such as multiobjective genetic algorithms [1] and multiobjective particle swarm optimization (MOPSO) [2]. On the other hand, research on the reliability-based multiobjective optimization (RBMO) is still developing [3–7]. Most studies selected the multiobjective GA, especially NSGA-II, as an optimizer.

However, computational efficiency of the multiobjective GA is not sufficient. This is because the multiobjective GA originally developed for design problem with discrete design variables and does not use the sensitivity information. A conventional single-objective reliability-based optimization [8] uses a gradient-based optimization method, because the sensitivity information is easily obtained from the reliability analysis such as the first-order reliability method (FORM). In addition, the efficient reliability-based design approach was developed to take consideration in using the gradient-based optimization method such as single-loop-single-vector (SLSV) method [9].

It is considered that the sensitivity information is also useful to the RBMO problem. Therefore, we proposed the computational efficient RBMO algorithms [10] by integrating the hybrid-type MOPSO [2] and the SLSV concepts [9]. The hybrid MOPSO has a constraint handling technique that uses the sensitivity of the constraints [11]. The constraint satisfaction technique consists of the two steps. First, the design candidate in infeasible region is forced to move to the feasible region on the basis of the violated constraint gradient information in each optimization step. Then, the constraint-satisfied design candidate is moved to the feasible boundary using bi-section method. For most engineering design problem, Pareto solutions generally lay on the feasible boundary. Therefore, the moved design candidate on the feasible boundary has higher possibility to select as a Pareto candidate. This strategy makes the Pareto searching efficiency improved, that was demonstrated through simple numerical design problem [11]. Then, the hybrid-type MOPSO with constraint satisfaction using sensitivity was applied to the RBMO problems [10, 12]. For computational efficiency, the method integrates the concept of SLSV method. The single-loop RBMO using the hybrid-type MOPSO was demonstrated to have higher computational efficiency [10, 12].

However, many calculateions were required until the candidate moves to feasible region for some cases with zigzag iterations as shown in Fig. 1. This study proposes the improvement method by eliminating such zigzag iterations based on an idea from the modified SLSV method [13, 14] or the conjugate mean value method [15] proposed for resolving the convergence problem for the reliability-based optimization. The original method only uses the sensitivity at the current position. On the other hand, the modified method uses sensitivities at the previous positions to improve the moving direction to the feasible regions. The efficiency of the proposed method

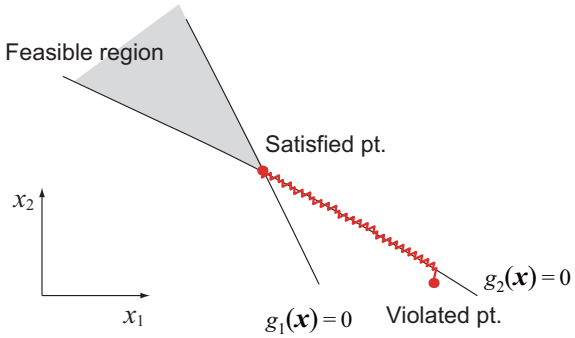

Figure 1: Feasible domain and example of moving paths to feasible boundary.

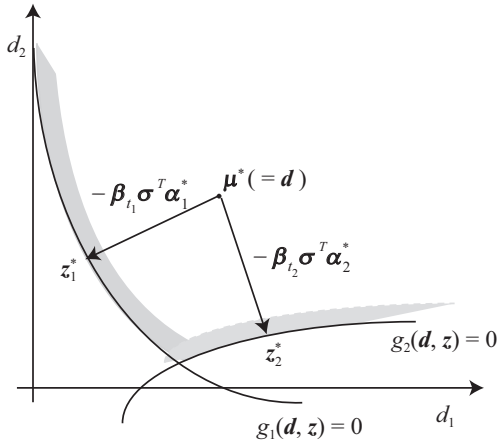

Figure 2: Relation between variables in applying SLSV.

is demonstrated through several design problems by investigating the convergence and diversity of finding Pareto optimal solutions.

4. Reliability-Based Multiobjective Optimization

Consider the multiobjective optimization problem subjected to the reliability constraints that consider uncertainties of design parameters such as material properties and applied loads. The limit state function that defines the j-th failure mode is denoted as $g_j(\boldsymbol{d},\boldsymbol{z})$ $(j=1,\cdots,k)$, where $\boldsymbol{d}=[d_1,\cdots,d_n]^T$ and $\boldsymbol{z}=[z_1,\cdots,z_l]^T$ are the design and random variables, respectively. The random variables are assumed to be independent from each other and denoted the mean value $\boldsymbol{\mu}=[\mu_1,\cdots,\mu_l]^T$ and the standard deviation as $\boldsymbol{\sigma}=\mathrm{diag}[\sigma_1,\cdots,\sigma_l]^T$. The failure probability P_{f_j} is defined as the probability that the j-th limit state function takes the negative value:

$$P_{f_j}=P(g_j(\boldsymbol{d},\boldsymbol{z})\le 0) \tag{1}$$

The reliability-based multiobjective optimization (RBMO) problem that minimize the multiple objective functions under the reliability constraints that the failure probabilities be lower than the prescribed values is formulated as follows:

$$\begin{aligned} &\text{Minimize:} && \boldsymbol{F}(\boldsymbol{d})=(f_1(\boldsymbol{d}),f_2(\boldsymbol{d}),\cdots,f_k(\boldsymbol{d})) \\ &\text{subject to:} && P_{f_j}=P(g_j(\boldsymbol{d},\boldsymbol{z})<0)\le\Phi(-\beta_{t_j}), \qquad (j=1,\cdots,m) \\ & && \boldsymbol{d}_L\le\boldsymbol{d}\le\boldsymbol{d}_U \end{aligned} \tag{2}$$

where $f_i(\boldsymbol{d})$ is the i-th objective function, β_{t_j} is the target reliability index for the j-th failure mode, $\Phi()$ is the standardized normal distribution function and $\boldsymbol{d}_U$ and $\boldsymbol{d}_L$ are the upper and lower bounds of design variables, respectively.

For the single-objective reliability-based optimization, the single-loop-single-vector method (SLSV) [9] is one of the approaches that reduce the excessive computational cost of the double-loop formulated problem that adopts the first order reliability method (FORM) as the reliability analysis. The key idea of the SLSV is that the reliability constraint is converted into the deterministic constraint by using a proper approximation of the design point, sometimes called most probable point (MPP). When the random vector $\boldsymbol{z}$ has a normal distribution $N(\boldsymbol{\mu},\boldsymbol{\sigma})$, the mean value $\boldsymbol{\mu}$ and the design point $\boldsymbol{z}_j$ of the j-th mode has following relationship as shown in Fig. 2. Note that the mean value vector μ is treated as design vector, $\boldsymbol{d}$ in this figure:

$$\begin{aligned} \boldsymbol{z}_j^* &= \boldsymbol{\mu}-\beta_{t_j}\boldsymbol{\sigma}^T\boldsymbol{\alpha}_j^*, \\ \boldsymbol{\alpha}_j^* &= \frac{\nabla g_j(\boldsymbol{d},\boldsymbol{z}_j^*)}{|\nabla g_j(\boldsymbol{d},\boldsymbol{z}_j^*)|} \end{aligned} \tag{3}$$

where $\boldsymbol{\alpha}_j$ is the unit gradient vector of the j-th limit state function with respect to random variables. This equation indicates that the current mean value $\boldsymbol{\mu}$ satisfying the target reliability index β_t will agree with the point that is β_t times the standard deviation depart from the design point, $\boldsymbol{z}_j^*$ in the opposite direction of $\boldsymbol{\alpha}_j^*$.

Based on the matter that the design point $\boldsymbol{z}_j^*$ lies on the limit state surface, the reliability constraint is rewritten as a following deterministic constraint:

$$g_j(\boldsymbol{d},\boldsymbol{\mu}-\beta_{t_j}\boldsymbol{\sigma}^T\boldsymbol{\alpha}_j^*)\ge 0 \tag{4}$$

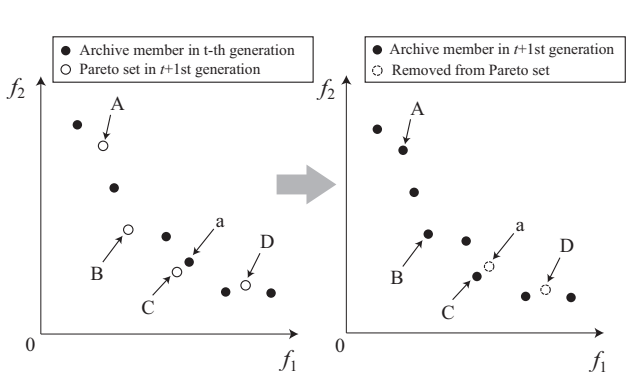

Figure 3: Selection of Pareto solutions in archive

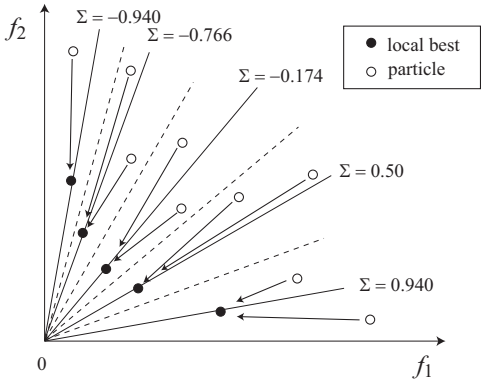

Figure 4: Global guide selection by sigma method

where the gradient vector $\boldsymbol{\alpha}_j^*$ should evaluate at the design point $\boldsymbol{z}_j^*$. However, the point is not known a prior. Therefore, a conventional RBDO method requires a iterated reliability analysis such as FORM. On the other hand, the SLSV method replaces the gradient vector $\boldsymbol{\alpha}_j^*$ by the gradient vector obtained in the previous optimization loop. This approximation makes the RBDO problem to a single loop algorithm.

5. Incorporation of Hybrid MOPSO with SLSV

In this study, the RBMO problem is solved by using the hybrid MOPSO [11] incorporated with concept of the SLSV method. The hybrid MOPSO has constraint handling capability using the gradient information of the constraint. Integration of the SLSV method into the constraint handling, the hybrid MOPSO is extended to the RBMO problem [10].

5.1 Multiobjective Particle Swarm Optimization (MOPSO)

The MOPSO is a kind of a heuristic approach of the multiple-point searching approach that expands to the multiobjective optimization from the particle swarm optimization (PSO). In the PSO, the current i-th design vector $\boldsymbol{d}_i^{t+1}$ is updated from the previous design $\boldsymbol{d}_i^t$ by using the velocity vector $\boldsymbol{v}_i^{t+1}$ as follows:

$$\begin{aligned} \boldsymbol{d}_i^{t+1} &= \boldsymbol{d}_i^t + \boldsymbol{v}_i^{t+1}, \\ \boldsymbol{v}_i^{t+1} &= w\boldsymbol{v}_i^t + C_1 r_1(\boldsymbol{d}_{p_i}^t - \boldsymbol{d}_i^t) + C_2 r_2(\boldsymbol{d}_{g_i}^t - \boldsymbol{d}_i^t) \end{aligned} \tag{5}$$

where $\boldsymbol{d}_{p_i}^t$ is called the personal best that is the best solution of the i-th design vector until the previous iteration, $\boldsymbol{d}_{g_i}^t$ is called the group best that is the best solution in all of the individuals. r_1 and r_2 are the uniform random variables in $[0, 1]$ to adjust the design update, w is called the inertial term and C_1 and C_2 are the parameters to adjust the effects of $\boldsymbol{d}_{p_i}^t$ and $\boldsymbol{d}_{g_i}^t$, respectively. In this study, $w = 0.4$ and $C_1 = C_2 = 2$ are adopted as the generally recommended value.

For the multiobjective optimization problem, the archive strategy is adopted as a kind of elitist method [16]. The method archives the Pareto candidate set and updates the set by comparing the current candidates with the archived candidates. As illustrated in Fig. 3, the current candidates A, B, and C are archived as new Pareto candidates, but the current candidate D and the archived candidate 'a' are removed because they are inferior to new Pareto candidates.

In the MOPSO, several methods were proposed to determine $\boldsymbol{d}_{\boldsymbol{p}_i}$ and $\boldsymbol{d}_{\boldsymbol{g}_i}$ which are called a local guide and a global guide, respectively, because the notion "best" is not suitable for the multiobjective optimization. This study adopts the sigma method [17] to determine the local and global guides. The sigma method evaluates the contribution rate between the objective functions as "sigma" by the following equation:

$$\Sigma = \frac{f_1^2 - f_2^2}{f_1^2 + f_2^2} \quad (\text{if } k = 2), \qquad \boldsymbol{\Sigma} = \frac{1}{\sum_{i=1}^{k} f_i^2} \begin{bmatrix} f_1^2 - f_2^2 \\ \vdots \\ f_{k-1}^2 - f_k^2 \\ f_k^2 - f_1^2 \end{bmatrix} \quad (\text{if } k \geq 3) \tag{6}$$

where Σ is a scholar for a bi-objective problem, and $\boldsymbol{\Sigma}$ becomes a vector for more than three objective function problem. As shown in Fig. 4, the Pareto candidate that has the most closest "sigma" value in the objective function space is selected as a global guide, $\boldsymbol{d}_{\boldsymbol{g}_i}^t$. This strategy is known to have a higher convergency and also higher diversity of Pareto solutions.

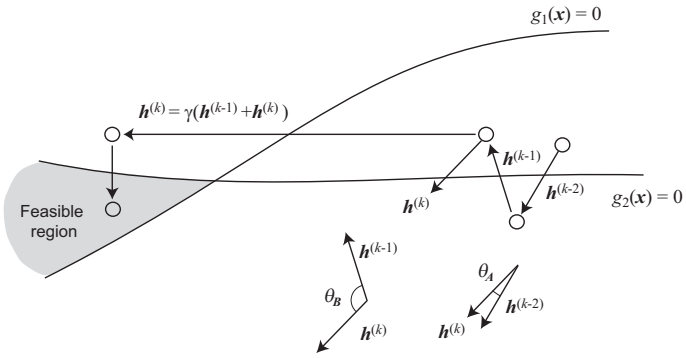

Figure 5: Image of zigzag elimination

On the other hand, as the number of archived Pareto candidates are increased, the archived strategy will take more computational time to compare and update the Pareto candidates. To save the computational effort, only one Pareto candidate in each prescribed sigma region is archived.

5.2 Constraint Handling Using Sensitivity and Zigzag Elimination

The constraint handling method proposed in our previous study [10–12] use the constraint sensitivity information. When the design candidate violates the constraints, it is moved to the feasible region to the direction obtained by using the violated constraint gradient information. When the violation is improved, the design candidate is moved to the same direction until the candidate satisfies the constrains. On the other hand, when the constraint violation is deteriorated, the moving direction is updated by evaluating the violated constraints and repeated until all of the constraints are satisfied. Finally, the candidates is moved to the feasible boundary using bi-section method. The method is found to have a sufficient Pareto optimal solution searching capacity for deterministic multiobjective optimization problem [11] and the RBMO problem integrated with the SLSV method [10, 12].

However, the method does not always worked well. When the violated constraints are often switched, the design candidate will approach the feasible region by zigzag as illustrated in Fig. 1. Such a case requires many iterations and therefore takes much computational effort.

We modify the method to eliminate the zigzag iterations. Several approaches were proposed for the single-objective reliability-based design optimization (RBDO) to improve the computational efficiency [13–15]. These methods use not the current sensitivity but the previous sensitivity to determine the searching direction. That is, if the searching direction is regarded as zigzag using the current and previous sensitivities, the direction is modified using the sensitivities.

An image of elimination of the zigzag iterations is shown in Fig. 5, where $\boldsymbol{h}$ indicates the moving direction vector based on the sensitivities of violated constraints and k is the number of iterations. First, the changing angles between successive searching directions are defined based on the Modified SLSV method [13] as follows:

$$\theta_A = \cos^{-1} \boldsymbol{h}^{(k-2)^T} \boldsymbol{h}^{(k)} \tag{7}$$

$$\theta_B = \cos^{-1} \boldsymbol{h}^{(k-1)^T} \boldsymbol{h}^{(k)} \tag{8}$$

That is, A and B are the angle between the current and the second previous searching directions, and the angle between the current and previous searching directions, respectively. respectively. Then, we decide that the zigzag occurred if $\theta_A < \theta_B$. In this case, the moving direction is modified using following equation:

$$\boldsymbol{h}^{(k)} = \gamma(\boldsymbol{h}^{(k-1)} + \boldsymbol{h}^{(k)}) \tag{9}$$

where γ is constant to adjust the magnitude of the moving direction. The flow of the constraint handling is illustrated in Fig. 6(a) and the algorithm is described as follows.

Step 1: Set step size Set the step size δ for the violated design $\boldsymbol{d}_i$.

Step 2: Set moving direction Evaluate the moving direction vector $\boldsymbol{h}$ using the gradient vectors of violated constraints $\nabla g_j(\boldsymbol{d}_i, \boldsymbol{d}_i - \beta_{t_j} \boldsymbol{\sigma}^T \boldsymbol{\alpha}_j^t)$ as follows.

$$\boldsymbol{h} = \sum_{j \in J} \frac{\nabla g_j(\boldsymbol{d}_i, \boldsymbol{d}_i - \beta_{t_j} \boldsymbol{\sigma}^T \boldsymbol{\alpha}_j^t)}{|\nabla g_j(\boldsymbol{d}_i, \boldsymbol{d}_i - \beta_{t_j} \boldsymbol{\sigma}^T \boldsymbol{\alpha}_j^t)|} \tag{10}$$

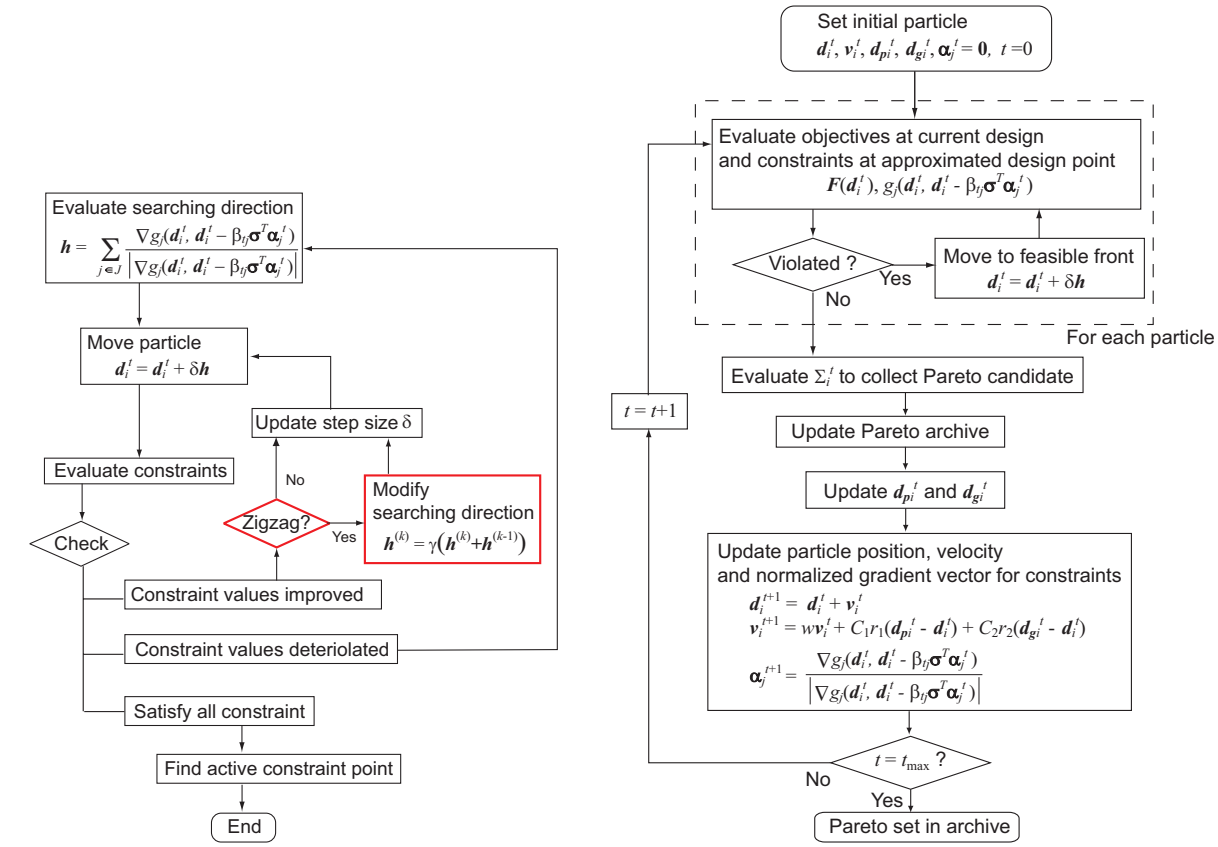

(a) Constraint satisfaction with eliminating zigzag iteration. (b) Reliability-based multiobjective optimization.

Figure 6: Computational flow of proposed hybrid-type MOPSO with constraint satisfaction.

where J indicates the violated constraint set J ($J = \{j | g_j(\boldsymbol{d}_i, \boldsymbol{d}_i - \beta_{t_j}\boldsymbol{\sigma}^T\boldsymbol{\alpha}_j^t) < 0, (j = 1, \cdots, m)\}$). Note that the reliability constraint is evaluated at the approximated design point $\boldsymbol{d} - \beta_{t_j}\boldsymbol{\sigma}^T\boldsymbol{\alpha}_j^t$, not the design variable $\boldsymbol{d}$ for using the concept of the SLSV method.

Step 3: Update design The design vector is updated using the vector $\boldsymbol{h}$ as follows:

$$\boldsymbol{d}_i = \boldsymbol{d}_i + \delta\boldsymbol{h} \tag{11}$$

Step 4: Judgment Evaluate all constraint conditions for the updated design vector. The next step is selected according to the following conditions.

In case that all of constraints are satisfied Go to Step 5.

In case that the violated constraint value is deteriorated Go back to Step 2 and update the moving direction, $\boldsymbol{h}$.

In case that the constraint value is improved Evaluate the changing angles in Eqs. (7) and (8). If $\theta_A \geq \theta_B$, then update the step size δ and go back to Step 3. Otherwise, modify the moving direction using the following equation:

$$\boldsymbol{h}^{(k)} = \gamma(\boldsymbol{h}^{(k-1)} + \boldsymbol{h}^{(k)}) \tag{12}$$

and then go back to Step 3. Where, γ is constant for adjusting the step size.

Step 5: Move to feasible boundary Move the feasible boundary ($g_j(\boldsymbol{d}_i, \boldsymbol{\mu} - \beta_t\boldsymbol{\sigma}^T\boldsymbol{\alpha}_j^t) = 0$) by applying bi-section method using the previous and the current design, where the previous design is violated and the current design is feasible.

The proposed algorithm is summarized in Fig. 6 (b). Feature of the proposed method is to update the normalized gradient vector of the reliability constraint $\boldsymbol{\alpha}_j^{t+1}$ at each step as well as the design vector and the velocity.

6. Numerical Examples

Efficiency of the proposed method is demonstrated through several engineering examples. The first example illustrates the computational efficiency of the zigzag elimination. Then, the efficiency of the improved hybrid-type MOPSO is swmonstrated through a couple of engineering example problems.

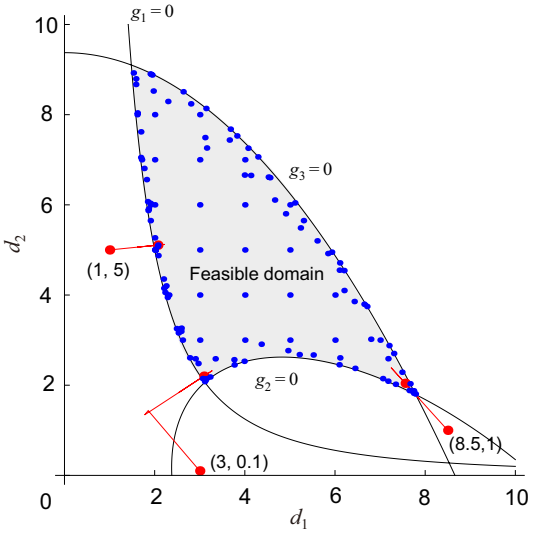

Figure 7: Feasible domain and results of enclosing.

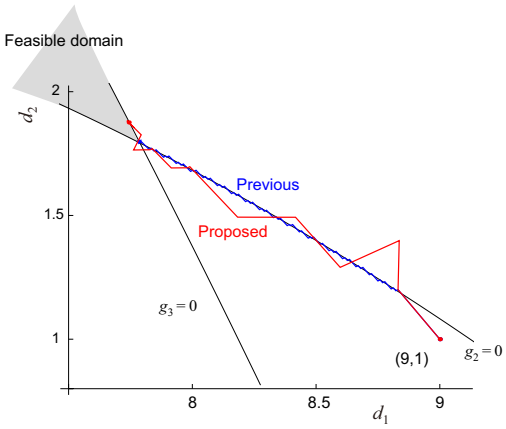

Figure 8: Effect of zigzag elimination process.

Table 1: Comparison of the number of function evaluations

	1-3	4-10	11-30	31-100	101-300	301-1000	Total	Average
Previous method	22	20	74	2	2	1	2226	18.4
Proposed method	22	20	76	2	1	0	1534	11.8

6.1 Efficiency of zigzag elimination

Consider the following feasible region consisting of convex and non-convex constraints [18]:

$$
\begin{aligned}
g_1(\boldsymbol{d}) &= \frac{d_1^2 d_2}{20} - 1 \geq 0 \\
g_2(\boldsymbol{d}) &= \frac{(d_1 + d_2 - 5)^2}{30} + \frac{(d_1 - d_2 - 12)^2}{120} - 1 \geq 0 \\
g_3(\boldsymbol{d}) &= \frac{80}{d_1^2 + 8d_2 + 5} - 1 \geq 0 \\
0 &\leq d_i \leq 10, \qquad (i = 1, 2)
\end{aligned}
\tag{13}
$$

Table 1 compares the number of function evaluations required for moving to the feasible region from the 121 starting grid points composed of integer coordinates that satisfies the side constraint, that is, (0,0) to (10, 10). In this example, the constant γ in Eq. (9) that adjusts the step size is set to 10. Though the previous method have 5 points that exceeds more than 100 function evaluations, the new method has only one point that the number is 102. The total number of function evaluations is reduced more than 30% from 2226 to 1534.

In Fig. 7, the blue dots are the final goal to the feasible region starting from the grid points and the red broken-lines are examples of the moving trajectories from several points. As a typical case, trajectories starting from (9,1) are compared in Fig. 8, where the blue broken-line corresponds to the previous method and the red one to the new method. For both method, the trajectories pass across a boundary of $g_2 = 0$ until satisfying all constraints. The previous method requires 245 function evaluations, but the new method requires only 60, about one-fourth.

6.2 Crashworthiness RBMO problem

The new method is applied to the crashworthiness RBMO problem [4] that is known as a benchmark problem comsisting of 2 objective functions and 9 constraint conditions in terms of 9 design variables. The random variables $\boldsymbol{x}$ follows independent normal distribution whose mean value are set as design variables $\boldsymbol{d}$ and the coefficient of variations are listed in Table 2 (a). The objective and constraint functions are also listed in Table 2 (b) and (c), respectively, that each function is formulated as polynomials through the response surface approximation.

In MOPSO, the number of particles is set as 100, the number of iterations 200 and $\gamma = 4$. Fig. 9 compares the Pareto set under the conditions that the target reliability indices β_t are set as 0, 3, and 6 between the previous and the new methods. Note that $\beta_t = 0$ corresponds to the deterministic problem. The obtained Pareto set for both methods are almost similar to the original one [4], though small difference exists only in the upper left part of the

Table 2: Formulation of crashworthiness RBMO problem [4].

(a) Design variables, side constraints, and cov in random variables

Name	Variable	Lower bound	Upper bound	COV(= σ/μ)
Thickness of B-pillar inner (mm)	d_1	0.5	1.5	0.03
Thickness of B-pillar reinforcement (mm)	d_2	0.5	1.5	0.03
Thickness of floor side inner (mm)	d_3	0.5	1.5	0.03
Thickness of cross members (mm)	d_4	0.5	1.5	0.03
Thickness of door beam (mm)	d_5	0.5	1.5	0.03
Thickness of door belt line reinforcement (mm)	d_6	0.5	1.5	0.03
Thickness of roof rail (mm)	d_7	0.5	1.5	0.03
Material yield stress for B-pillar inner (GPa)	d_8	0.192	0.750	0.02
Material yield stress for floor side inner (GPa)	d_9	0.192	0.750	0.02

(b) Two Objective functions

Weight	$f_1 = 1.98 + 4.9d_1 + 6.67d_2 + 6.98d_3 + 4.01d_4 + 1.78d_5 + 2.73d_7$
Door velocity	$f_2 = 16.45 - 0.489d_3d_7 - 0.843d_5d_6$

(c) Nine Constraints

Name		Upper limit	Formulation
Abdomen load (kN)	g_1	1.0	$1.163 - 0.3717x_2x_4 - 0.484x_3x_9$
Rib deflection upper (mm)	g_2	28.0	$28.98 + 3.818x_3 - 4.2x_1x_2 + 6.63x_6x_9 - 7.70x_7x_8$
Rib deflection middle (mm)	g_3	30.0	$33.86 + 2.95x_3 - 5.057x_1x_2 - 11.0x_2x_8 - 9.98x_7x_8 + 22.0x_8x_9$
Rib deflection lower (mm)	g_4	38.0	$46.36 - 9.9x_2 - 12.9x_1x_8$
Public symphysis force (kN)	g_5	4.4	$4.72 - 0.5x_4 - 0.19x_2x_3$
B-Pillar velocity (m/s)	g_6	10.0	$10.58 - 0.674x_1x_2 - 1.95x_2x_8$
VC upper (m/s)	g_7	0.28	$0.261 - 0.0159x_1x_2 - 0.188x_1x_8 - 0.019x_2x_7 + 0.0144x_3x_5 + 0.08045x_6x_9$
VC middle (m/s)	g_8	0.32	$0.214 + 0.00817x_5 - 0.131x_1x_8 - 0.0704x_1x_9 + 0.031x_2x_6 - 0.018x_2x_7$ $+0.021x_3x_8 + 0.121x_3x_9 - 0.00364x_5x_6$
VC lower (m/s)	g_9	0.35	$0.74 - 0.61x_2 - 0.163x_3x_8 - 0.18x_7x_9 + 0.227x_2x_2$

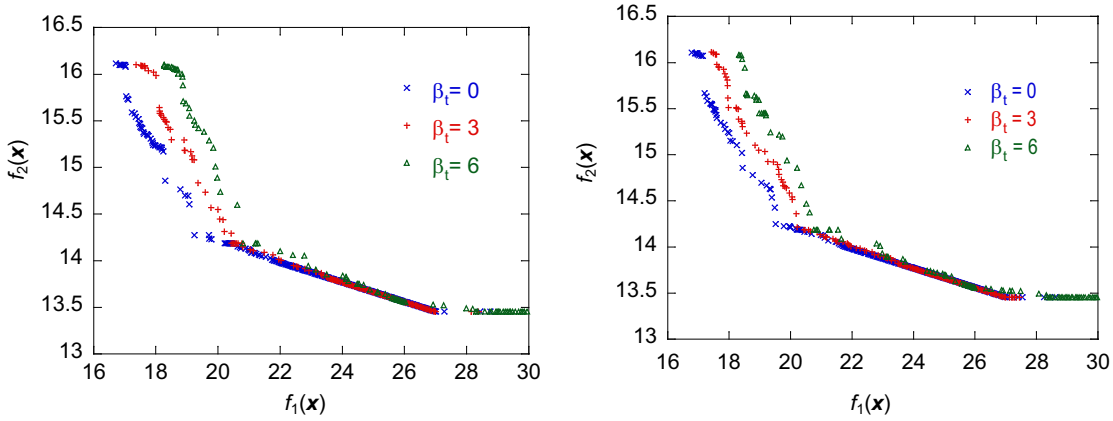

(a) Previous method (b) Proposed method

Figure 9: Pareto set comparison for crashworthiness RBMO problem.

Table 3: Computational performance of crashworthiness RBMO problem.

Target reliability β_t	Previous Number of evaluations	Ratio	Proposed Number of evaluations	Ratio
0	748310	18.71	688263	17.21
3	743607	18.59	695454	17.39
6	999755	24.99	873327	21.83

Pareto set. The total number of function evaluations and the average number of evaluations per each particle in each iteration are compared in Table 3. Though the improvement is not so large in this example, the new method slightly reduces the number of function evaluations.

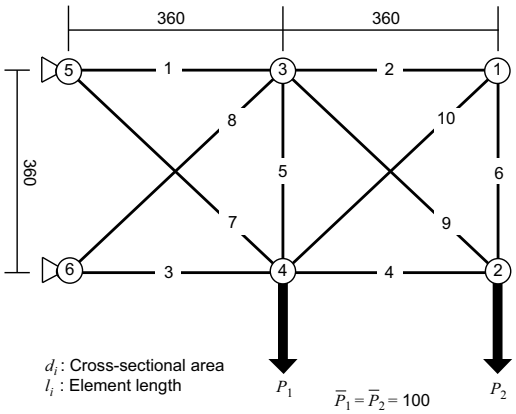

Figure 10: Ten-bar truss design problem

Table 4: Formulation of 10-bar truss design problem [4].

(a) Design and random variables

Design variables d_i	Cross-sectional area	$0.1 \le d_i \le 5$,	$(i = 1, \cdots, 10)$
Random variables x_i	Tensile strength	$N(25, 2.5)$,	$(i = 1, \cdots, 10)$
	Compression strength	$N(-25, 2.5)$,	$(i = 11, \cdots, 20)$
	Applied load	$N(100, 10)$,	$(i = 21, 22)$

(b) Reliability constraints

Tensile	$P(x_i - \sigma_i \le 0) \le \Phi(-\beta_t)$,	$(i = 1, \cdots, 10)$,	(if $\sigma_i \ge 0$)
Compression	$P(\sigma_i - x_i \le 0) \le \Phi(-\beta_t)$,	$(i = 11, \cdots, 20)$,	(if $\sigma_i \le 0$)

6.3 10-bar truss design problem

This example is extended from a typical 10-bar truss design problem as shown in Fig. 10 that is known as a single-objective benchmark problem [13]. The member cross-sectional areas are treated as design variables, $d_i, (i = 1, \cdots, 10)$ and the two nodal applied loads and member allowable stresses are adopted as independent normal distributed random variables as listed in Table 4 (a). The two objective functions is defined to minimize the total volume and the tip displacement. The reliability constraints are formulated that the reliability which the member stress does not exceed the allowable stress should be higher than the target reliability as listed in Table 4 (b). This RBMO problem consists of the two objectives and 20 reliability constraints with 10 design variables and 22 random variables. Other properties such as the member length, $l_i, (i = 1, \cdots, 10)$, and Young's modulus, $E = 2 \times 10^5$, are treated as deterministic values.

Note that this problem adopts the deterministic design variables, that is, μ, the mean value of random variables in the second argument of Eq. (4) does not correspond to design variable. The concept of SLSV is applicable even in this case, though the design point $\boldsymbol{z}_j^*$ described in Fig. 2 is not rigorously correct.

In MOPSO, the number of particles is set as 100, the number of iterations 200 and $\gamma = 4$. Fig. 11 compares the Pareto set under the conditions that the target reliability indices β_t are set as 0, 3, and 6 between the previous and the new methods. The new method achieves the diversity of Pareto set. On the other hand, the previous method does not obtain the lower right region of the Pareto set.

The lower right region of Pareto set corresponds to design with smaller tip displacement but larger volume as shown in Fig. 12 (a). As this kind of design does not have active reliability constraints, the difference between the target reliability indices does not appear. On the other hand, the upper left region of Pareto set is much different from the above design. The configuration is shown in Fig. 12 (b), where the design with minimum volume but has larger tip displacement. As the reliability constraints are active around this region, the target reliability has significant effect on the Pareto solutions. Both configurations are not suitable from the viewpoint of mechanical engineering. The design configuration corresponding to the central area in the Pareto curve is shown in Fig. 12 (c). This configuration has a good balance between the volume and the tip displacement and is similar to the typical design of the single-objective optimization problem that minimize the volume under the tip displacement and member stress constraints.

Finally, the computational effort is compared in Table 5. It is found that the new method reduces the number of function evaluations as much as about 60% of the previous method in this example.

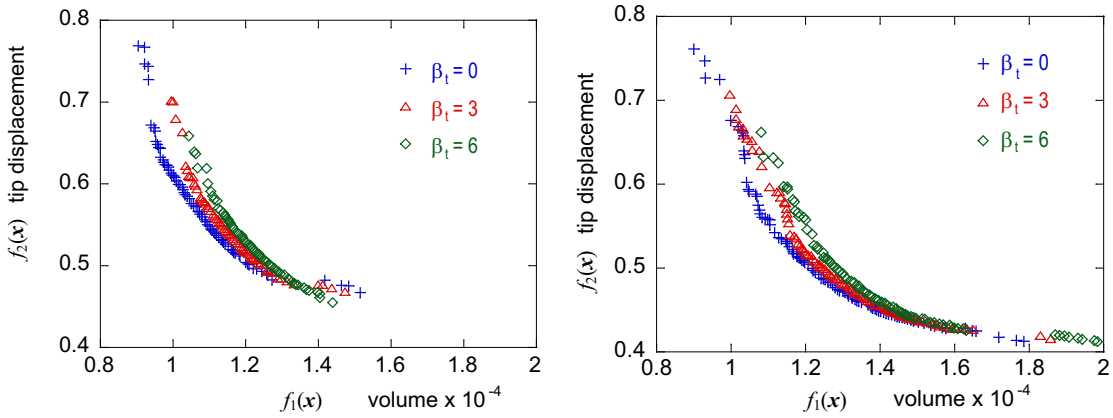

(a) Previous method (b) Proposed method

Figure 11: Pareto set comparison for crashworthiness RBMO problem.

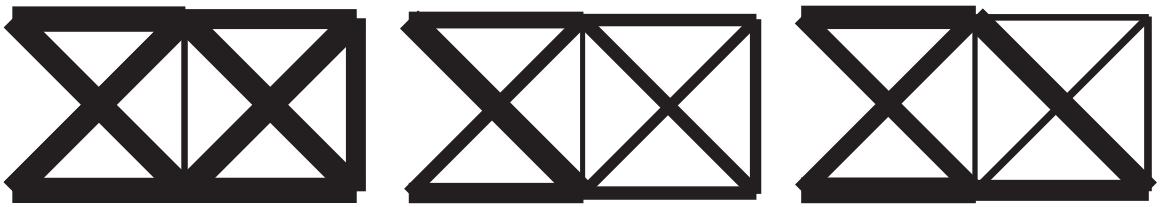

(a) Displacement minimization design (b) Volume minimization design (c) Intermediate design

Figure 12: Typical Pareto optimum configurations of 10-bar truss.

Table 5: Computational performance of 10-bar truss RBMO problem.

Target reliability β_t	Previous Number of evaluations	Ratio	Proposed Number of evaluations	Ratio
0	830779	41.54	512767	25.64
3	1064178	53.21	620221	31.01
6	1364916	68.25	801103	40.06

7. Conclusion

This study proposes the improvement method of the hybrid-type MOPSO that the authors developed for the multiobjective optimization formulated as continuous design variables and the RBMO [10–12]. The hybrid MOPSO integrates the constraint satisfaction technique using gradient information of constraints. The constraint satisfaction technique consists of two functions: moving the design candidate with constraint violation to the feasible region using sensitivity information of the violated constraints and to the feasible boundary using bi-section method. Some design candidates require huge numbers of iterations until the candidate moves to feasible region, when the violated constraint conditions are shifted frequently during the constraint satisfaction process. Because the original method only uses the sensitivity at the current position,

In order to eliminate such zigzag iterations, an idea from the modified SLSV method or the conjugate mean value method [13, 14] is applied. The improved method uses sensitivities at the previous positions to improve the moving direction to the feasible regions.

The efficiency of the proposed method is demonstrated through several design problems by investigating the convergence and diversity of finding Pareto optimal solutions.

References

[1] K. Deb, A. Pratap, S. Agarwal and T. Meyarivan, A Fast and Elitist Multiobjective Genetic Algorithm:NSGA-II, *IEEE Trans. Evol. Comput.*, 6(2), 182-197, 2002.

[2] M. Reyes-Sierra and C. A. Coello Coello, Multi-Objective Particle Swarm Optimizers: A Survey of the State-of-the-Art, *Int. J. Comput. Intell. Res.*, 2(3), 287-308, 2006.

[3] K. Deb, D. Padmanabhan, S. Gupta and A. K. Mall, Reliability-Based Optimization Using Evolutionary Algorithms, *IEEE Trans. Evo. Opt.*, 13(5), 1054-1074, 2009.

[4] K. Sinha, Reliability-based multiobjective optimization for automotive crashworthiness and occupant safety, *Struct. Multidisc. Optim.*, 33(3), 255-268, 2007.

[5] F. Li, Z. Luo and G. Sun, Reliability-Based Multiobjective Design Optimization under Interval Uncertainty, *Comput. Model. Eng. Sci.*, 74(1), 39-64, 2011.

[6] S. Rangavajhala and S. Mahadevan, Joint Probability Formulation for Multiobjective Optimization Under Uncertainty, *J. Mech. Design*, 133, 051007, 2011.

[7] J. Greiner and P. Hajela, Truss Topology Optimization for Mass and Reliability Considerations – Co-Evolutionary Multiobjective Formulations, *Struct. Multidisc. Optim.*, 45(4), 589-613, 2012.

[8] I. Enevoldsen, Reliability-Based Structural Optimization, *Structural Reliability Theory*, 87, 1991.

[9] X. Chen, T. K. Hasselman and D. J. Neill, Reliability Based Structural Design Optimization for Practical Applications, *Proc. 38th AIAA SDM Conf.*, AIAA-97-1403, 1997.

[10] N. Kogiso, S. Kawaji, M. Ohara, A. Ishigame and K. Sato, Reliability-Based Multiobjective Optimization Using Hybrid-type Multiobjective PSO Algorithms Incorporating Sensitivity Analysis on Constraint Condition, *Trans. JSME, C*, 78(790), 2229-2240, 2012, (*in Japanese*).

[11] N. Kogiso, S. Kawaji, M. Ohara, A. Ishigame and K. Sato, Constraint Handling in Multiobjective Particle Swarm Optimization Incorporating Sensitivity Analysis on Constraint Condition. *Trans. JSME, C*, 78(785), 201-213, 2012, (*in Japanese*).

[12] S. Kawaji, N. Kogiso, M. Ohara, A. Ishigame and K. Sato, Validity of Reliability-Based Multiobjective Optimization Incorporated MOPSO with SLSV, *7th China-Japan-Korea Joint Symposium on Optimization of Structural and Mechanical Systems*, J-22, 2012.

[13] N. Kogiso, Y. S. Yang, B. J. Kim, and and J. O. Lee, Modified Single-Loop-Single-Vector Method for Efficient Reliability-Based Design Optimization, *J. Adv. Mech. Des. Syst.*, 6(7), 1206-1221, 2012.

[14] J. O. Lee, Y. S. Yang, and W. S. Ruy, A Comparative Study on Reliability-Index and Target Performance-Based Probabilistic Structural Design Optimization, *Comput. Struct.*, 80(3-4), 257-269, 2002.

[15] B. D. Youn, K. K. Choi, and Y. H. Park, Hybrid Analysis Method for Reliability-Based Design Optimization, *J. Mech. Design*,125(2), 221-232, 2003.

[16] J. D. Knowles and D. W. Corne, Approximating the Nondominated Front using Pareto Archived Evolution Strategy, *Evol. Comput.*, 8(2), 149-172, 2000.

[17] S. Mostaghim and J. Teich, Strategies for Finding Good Local Guides in Multi-Objective Particle Swarm Optimizetion, *Proc. IEEE Swarm Intelligence Symp.*, 26-33, 2003.

[18] J. Liang, Z. P. Mourelatos, and J. Tu, A Single-Loop Method for Reliability-Based Design Optimization, *ASME 2004 IDETC/IEC*, ASME DETC 2004-57255, 2004.